Isotope effects on exciton energies in CdS

J. M. Zhang,* T. Ruf, R. Lauck, and M. Cardona
Max-Planck-Institut für Festkörperforschung, Heisenbergstrasse 1, D-70569 Stuttgart, Germany
(Received 25 September 1997)

The energies of free and bound excitons related to the *A* and *B* valence bands in isotopically pure wurtzite CdS (^{110}CdS, ^{112}CdS, ^{114}CdS, ^{116}CdS) and natural CdS have been measured at low temperature by means of photoluminescence, piezomodulated reflectivity, and photomodulated reflectivity. With an increase of the Cd mass the excitonic energies increase by about 40–68 μeV/amu, one order of magnitude less than observed when increasing the S mass. These results can be understood from the point of view of electron-phonon interaction, provided one takes into account the 4*d* electrons of Cd that hybridize in the valence band with the 3*p* states of sulfur. The results are compared with existing experimental data of the temperature-dependent excitonic energies in CdS. [S0163-1829(98)06216-X]

I. INTRODUCTION

Much attention is presently being paid to isotope effects in semiconductors.[1] Since the frequencies and amplitudes of lattice vibrations depend directly on the atomic mass, isotope substitution in crystals is expected to have a significant influence on lattice-dynamical and related properties, e.g., phonon frequencies, linewidths and lifetimes, lattice parameters, thermal expansion, and thermal conductivity.[1] Investigations of these isotopic-mass-dependent properties have been extensively performed in elemental group-IV diamond-type semiconductors during the last few years.[1] They have also recently been extended to compound semiconductors.[2–5] Modifications of phonon properties also influence the electronic states of a semiconductor via the electron-phonon interaction and changes in the lattice parameters (''thermal expansion'').[1] This occurs when either the temperature or the isotopic mass of atoms is varied.[1,6] Besides the anharmonic thermal-expansion term, which exists even at $T=0$ because of the ''zero-point'' motion, the main contribution to the band-gap renormalization comes from the electron-phonon interaction, which can be further separated into Debye-Waller and self-energy terms.[7] Along these lines, the temperature dependence of band gaps and other critical points in elemental and binary semiconductors has been investigated in numerous experimental and theoretical studies.[7–9] Some work has also been performed on the dependence of gap shifts on isotopic mass in elemental group-IV diamond-type semiconductors.[10–13] The recent availability of high-quality isotopically pure samples has opened the door to investigations of the isotopic-mass dependence of the electronic structure and its relation to the electron-phonon interaction also in compound semiconductors.[2,14–16]

In compounds, the lattice vibrations involve combinations of displacements of the individual constituents, and the phonon branches in the Brillouin zone therefore exhibit different isotope shifts. In addition, the valence- and conduction-band states are usually combinations of the atomic orbitals of various constituent elements. Selective isotope substitution in compounds thus allows one to investigate the behavior of specific phonons and their contribution to the gap renormalization,[15] as well as the hybridization of the electronic energy bands.[2,14]

In the present paper we investigate several wurtzite CdS samples made from natural and isotopically pure Cd between ^{110}Cd and ^{116}Cd. The energies of the free and bound excitons of the *A* and *B* bands have been measured with photoluminescence (PL), photomodulated reflectivity (PR), and piezomodulated reflectivity (PzR). The exciton energies increase with increasing Cd mass. The rate of change $\partial E/\partial M_{\mathrm{Cd}}$, however, is significantly smaller than that observed when increasing the S mass.[17] This very small value is interpreted in terms of *p-d* band mixing and electron-phonon interaction. The temperature dependence measured for the excitonic energies is consistent with the corresponding isotope effects.

II. EXPERIMENT AND RESULTS

The measurements were performed on several CdS samples grown by vapor transport at about 1000 K in an argon atmosphere with isotopically pure ^{110}Cd, ^{112}Cd, ^{114}Cd, and ^{116}Cd and natural sulfur $^{\mathrm{nat.}}$S (mass 32.066). A natural sample $^{\mathrm{nat.}}$Cd$^{\mathrm{nat.}}$S ($^{\mathrm{nat.}}$Cd mass 112.411) was prepared under the same conditions as a reference. The samples are the same as those used in Ref. 3. The specimen have the shape of thin plates with the *c* axis in the surface in a direction parallel to the longer sides. Their typical thickness is around 0.3 mm. This requires paying special attention to strain effects, which can easily be introduced on the thin samples when mounting them in the cryostat. For the PL and PR measurements, only one end of the samples was fixed on a copper sample holder while the other side was not attached and thus stress free. Only areas without strain were used for the measurements.

For the PzR measurements, the samples were mounted onto a piezoelectric transducer (Phillips PXE 5) using Si vacuum grease at either end along the long edge (the direction of the *c* axis of our samples).[18] Only the ^{112}CdS sample had a sufficiently large size so that it was not strained due to mounting it onto the piezoelectric transducer. We verified this point from the measured peak energies compared with those from PR and PL measurements. The strain modulation to which the samples were subjected was generated by the

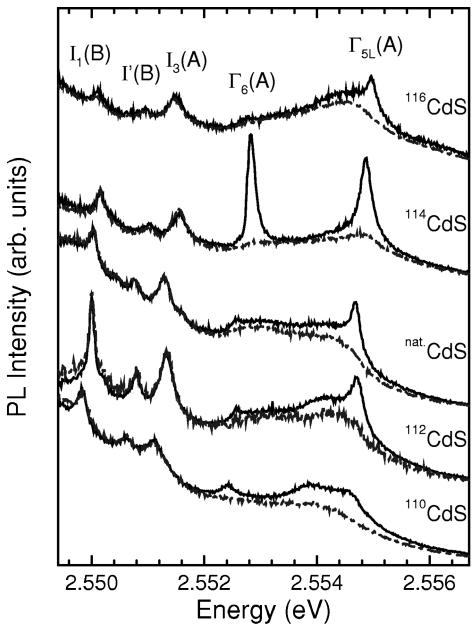

FIG. 1. Photoluminescence (PL) spectra of CdS grown with isotopically pure and with natural Cd (as indicated in the figure) in the energy region of the A excitons. The measurements were performed at 8 K with $\mathbf{k}\perp\mathbf{c}$, $\mathbf{E}\perp\mathbf{c}$ (dashed-dotted lines) and $\mathbf{E}\|\mathbf{c}$ (solid lines). The intensities have been normalized so that the three peaks at the left side have the same height.

alternating expansion of the transducer driven by a unipolar modulation voltage (f = 400 Hz, $V_{p\text{-}p}$ = 275 V) from a Kepco high-voltage operational amplifier. Details of the PzR technique can be found in Refs. 18 and 19.

The 2.6-eV laser line from an Ar^+-ion laser was used as the excitation for PL measurements. This line was modulated with a 90-Hz chopper when measuring PR spectra. A 50 W tungsten-halogen lamp was used as the source of the reflected light. The PL signals were dispersed with an 0.85-m SPEX double monochromator and detected with a GaAs photomultiplier. The modulated reflected light was dispersed by the same monochromator and detected with a Si diode, followed by a lock-in amplifier and a computer. All measurements were taken at 6 to 8 K with the samples inside a flow-through helium cryostat. To measure the small energy differences between the isotopically modified samples, high resolution was obtained by using very narrow slit widths. An emission peak from a neon lamp was always measured simultaneously with the spectrum to obtain a precise calibration of the energy scale.

In order to determine the energy positions associated with the various observed excitonic structures, the modulation spectra were fitted to the derivative of the Lorentzian line

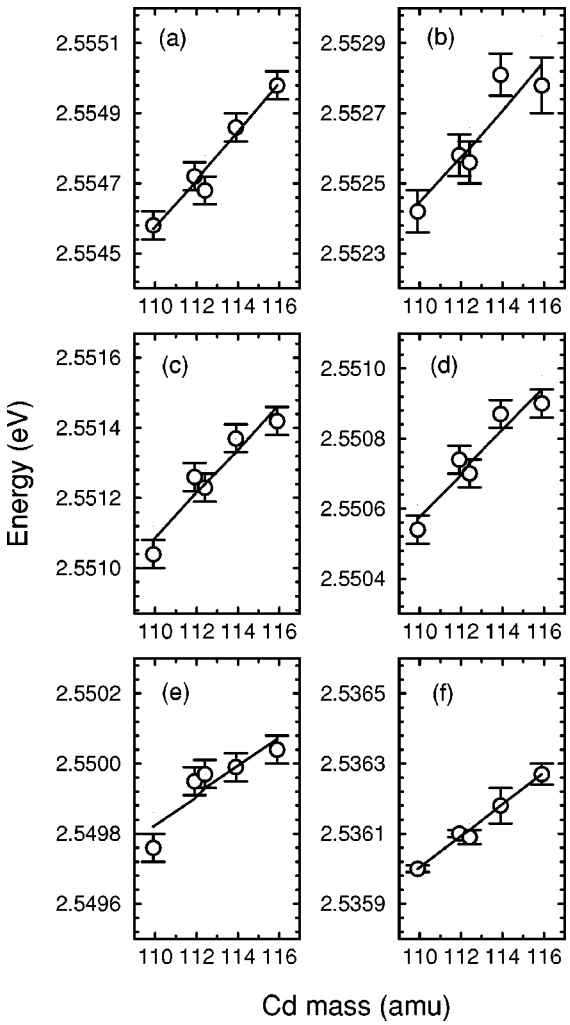

FIG. 2. Cd mass dependence of the (a) $\Gamma_5^L(A)$, (b) $\Gamma_6(A)$, (c) $I_3(A)$, (d) $I'(B)$, (e) $I_1(B)$, and (f) $I_1(A)$ excitons obtained from PL measurements at 8 K. The solid lines are the best linear fit to the data.

shape with the functional form[20]

$$\frac{\Delta R}{R}=\mathrm{Re}\left[\sum_j C_j e^{i\theta_j}(E-E_j+i\Gamma_j)^{-n}\right], \tag{1}$$

where C_j, θ_j, E_j, and Γ_j are the amplitude, phase, energy, and the broadening parameter of the jth oscillator, respectively. The exponent n equals 2 in the present case, corresponding to bulk excitons.[20]

The properties of excitons and excitonic polaritons in natural CdS have been extensively investigated in the literature.[21] Wurtzite CdS has three valence bands and one

TABLE I. Isotope shifts of the excitonic energies in CdS for Cd substitution measured in the present work compared with the results for S substitution extracted from reflectivity spectra in Ref. 17 ($T\approx 6$ K). The slopes are given in units of μeV/amu.

	PL						PR	
Exciton	$\Gamma_5^L(A)$	$\Gamma_6(A)$	$I_3(A)$	$(I'B)$	$I_1(A)$	$I_1(B)$	$\Gamma_5^L(A)$	$\Gamma_5^L(B)$
$\partial E/\partial M_{\mathrm{Cd}}$	68 ± 13	68 ± 20	63 ± 13	61 ± 13	45 ± 7	43 ± 13	61 ± 20	40 ± 22
$\partial E/\partial M_{\mathrm{S}}$							740 ± 100	740 ± 100

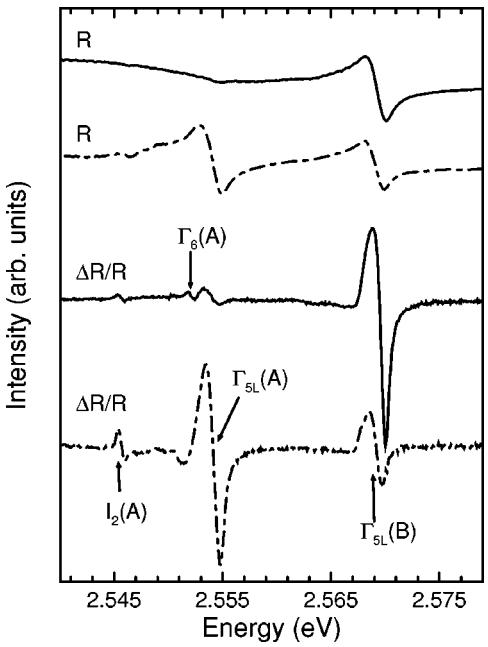

FIG. 3. Reflectivity (R) and piezomodulated reflectivity ($\Delta R/R$) spectra of ^{112}CdS at 8 K recorded with $\mathbf{k}\perp\mathbf{c}$ for $\mathbf{E}\perp\mathbf{c}$ (dashed-dotted lines) and $\mathbf{E}\parallel\mathbf{c}$ (solid lines), respectively.

conduction band with symmetries Γ_9 (A band), Γ_7 (B band), Γ_7 (C band), and Γ_7 (conduction band), respectively. The intrinsic states of the corresponding excitons follow from the decomposition of the product representation $\Gamma_{9v}\times\Gamma_{7c}=\Gamma_5+\Gamma_6$ for A excitons and $\Gamma_{7v}\times\Gamma_{7c}=\Gamma_1+\Gamma_2+\Gamma_5$ for both B and C excitons. Transitions to the Γ_5 states are dipole allowed for $\mathbf{E}$ perpendicular to the c axis, those to Γ_1 are possible with $\mathbf{E}$ polarized parallel to the c axis. The Γ_5 excitons are split into Γ_5^T and Γ_5^L branches when coupled with photons (excitonic polariton) that correspond to the transverse and the longitudinal components, respectively.

We show in Fig. 1 the PL spectra of the isotopically pure and natural CdS samples in the energy region of the free A excitons measured at 8 K. The solid and dashed lines are obtained with $\mathbf{E}\parallel\mathbf{c}$ and $\mathbf{E}\perp\mathbf{c}$, respectively. The wave vector $\mathbf{k}$ is kept perpendicular to $\mathbf{c}$ in these measurements (with the incident and outgoing light normal to the surface). The intensities of the spectra measured with $\mathbf{E}\parallel\mathbf{c}$ have been renormalized so as to obtain similar intensities of the three peaks on the left side of the figure. Following Ref. 21 and references therein, we assign the peaks from high to low energy to the $\Gamma_5^L(A)$ and $\Gamma_6(A)$ free excitons, excitons bound to ionized donors $[I_3(A)]$, and to two excitons bound to neutral acceptors derived from the B band $[I'(B)$ and $I_1(B)]$, respectively. The peak positions of the free excitons can be better fitted from the difference spectra between the two polarizations. We also observed several peaks in the energy region of the A-band bound exciton, such as the neutral donor line $I_2(A)$, which are difficult to distinguish and therefore hard to compare from sample to sample. However, only one sharp peak was observed in the energy region of the exciton bound to neutral acceptors $[I_1(A)]$. This allows the comparison of the energy of this exciton among different samples.

Figure 2 shows the energy positions of various excitons as a function of the Cd mass. All the peaks shift towards higher energy when Cd is substituted by a heavier isotope. Over this small range of Cd masses (from 110 to 116), the variation of the excitonic energies can be approximated by a linear function, i.e., $E=E_{110}+(\partial E/\partial M_{\mathrm{Cd}})(M_{\mathrm{Cd}}-M_{110})$, where E_{110} and M_{110} represent the gap energy and the Cd mass in ^{110}CdS, respectively. Fits of this formula to the experimental data by a least-squares procedure yield the slopes $\partial E/\partial M_{\mathrm{Cd}}$ listed in Table I.

Figure 3 shows the reflectivity and PzR spectra of ^{112}CdS measured with $\mathbf{E}$ parallel and perpendicular to the c axis. Structures related to the A and B excitons follow the standard wurtzite selection rules. The A-band free exciton [including the $I_2(A)$ bound exciton structure around 2.5453 eV which is associated with the A band] is only observed when $\mathbf{E}\perp\mathbf{c}$, while the free B exciton is observed for both $\mathbf{E}\perp\mathbf{c}$ and $\mathbf{E}\parallel\mathbf{c}$. Consistent with the PL spectra, the $\Gamma_6(A)$ exciton is not completely forbidden. In second-order perturbation theory the $\Gamma_6(A)$ state is mixed with $\Gamma_1(B)$ for finite wave vectors[21] when $\mathbf{E}\parallel\mathbf{c}$; it is therefore clearly seen in the $\mathbf{E}\parallel\mathbf{c}$ configuration in which the nearby $\Gamma_5(A)$ oscillator is forbidden.

The PR spectra of the isotopic samples measured at 6 K with $\mathbf{E}\perp\mathbf{c}$ are shown in Figs. 4(a) and 4(b) in the energy regions of A and B excitons, respectively. The split transverse component of the $\Gamma_5(B)$ exciton is clearly observed in ^{112}CdS and $^{\mathrm{nat.}}$CdS where the excitons have small inhomogeneous broadening because of the higher sample quality. In the other specimen these two spectral structures are broader. Fits of the spectra using Eq. (1) are given by the solid lines. They always involve two oscillators whose fitted energy positions are marked in Fig. 4 by the vertical lines. The energies of the $\Gamma_5^T(A)$ excitons are not shown in Fig. 4(a) since the rather broad and featureless spectra in this range make it hard to determine them accurately. With an increase of the Cd mass the excitonic energies shift to higher values. These energy shifts are shown in Figs. 5(a) and 5(b) for the A and B excitons (Γ_5^L), respectively. A least-squares fit yields the slopes for the A and B excitons which are also listed in Table I.

We also found excited states of the A and B excitons; they are shown in the PR spectra of Fig. 6. Polarization measurements indicate that the features at about 2.574 eV and 2.590 eV arise from A- and B-exciton transitions to the $n=2$ excited states ($2s$), respectively. This allows us to directly determine the binding energy (E_b) and the corresponding band gaps (E_g) from a hydrogenlike model:[22]

$$E_n=E_g-E_b/n^2. \tag{2}$$

In this manner, we obtain binding energies of A excitons of 26.4 ± 0.2 meV and 26.8 ± 0.2 meV in ^{112}CdS and $^{\mathrm{nat.}}$CdS, respectively. The corresponding band gaps E_g ($\Gamma_{7c}-\Gamma_{9v}$) are, as denoted in Fig. 6 by $n=\infty$, 2.5806(2) eV and 2.5809(2) eV, respectively. In the case of B excitons, these values are E_b = 27.1 ± 0.2 meV (27.1 ± 0.2 meV) and E_g ($\Gamma_{7c}-\Gamma_{7v}$) = 2.5964(2) eV [2.5963(2) eV] for the ^{112}CdS [$^{\mathrm{nat.}}$CdS] sample. Unfortunately, the $n=2$ excited states of the A and B excitons could not be observed in the other isotopic CdS samples. Better samples are required for such measurements.

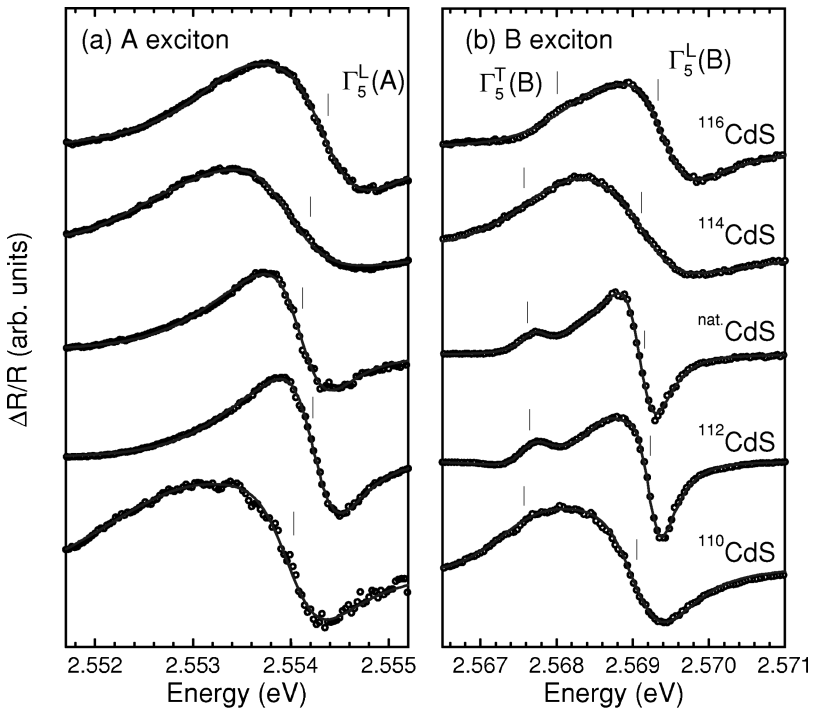

FIG. 4. Photoreflectance (PR) spectra of CdS grown with isotopically pure and with natural Cd (as indicated in the figure) in the energy region of the free A (a) and B exciton (b) ground state, respectively. The measurements were performed at 6 K with $\mathbf{k}\perp\mathbf{c}$ and $\mathbf{E}\perp\mathbf{c}$. The open circles are experimental data and the solid lines represent fits using Eq. (1).

III. DISCUSSION

Band-gap energies shift with a change of temperature or isotope substitution. Both effects can be understood in the light of the renormalization of electronic states by lattice vibrations.[1,6] In addition to the thermal expansion [changes in the crystal volume (or the lattice constants) due to changes of either temperature or atomic masses], band gaps are renormalized through the electron-phonon interaction at constant volume. This contribution can be further separated into the so-called Debye-Waller terms (DW, interaction between one electron and two phonons in first-order perturbation theory) and the Fan or self-energy terms (SE, interaction between one electron and one phonon taken to second order in perturbation theory). The electron-phonon interaction renormalization of a band gap $E_{n\mathbf{k}}$ can be expressed as a sum over phonons:[6,10,15]

$$\Delta E_{n\mathbf{k}}=\sum_{\mathbf{q},j}\left(\frac{\partial E_{n\mathbf{k}}}{\partial n_{\mathbf{q}j}}\right)\left(n_{\mathbf{q}j}+\frac{1}{2}\right), \tag{3}$$

where $n_{\mathbf{q}j}$ is the Bose-Einstein occupation number $[\exp(\hbar\omega_{\mathbf{q},j}/k_BT)-1]^{-1}$ of the vibrational mode with wave vector $\mathbf{q}$ and branch index j. The coefficients $\partial E_{n\mathbf{k}}/\partial n_{\mathbf{q}j}$ can, in principle, be calculated by evaluating the DW and SE terms, provided a realistic lattice-dynamical calculation, giving reasonable values of both phonon frequencies and eigenvectors, is available. Along these lines, numerous calculations have been performed aiming at predicting the temperature and isotopic mass dependence of the electronic structure and its relation to electron-phonon interaction in semiconductors with both monoatomic diamond-type and binary zinc-blende structures.[7–10,15] Unfortunately, such calculations are not available for wurtzite-type materials such as CdS.

For GaAs or ZnSe, isotope substituents of either type should lead to shifts of the E_0 gap which have been calculated to be 430 (420) and 310 (300) μeV/amu for cation (anion) mass replacement, respectively.[15] These values are in reasonable agreement with data measured for GaAs $[\partial E_0/\partial M_{\mathrm{Ga}} = 390(60)\ \mu\mathrm{eV/amu}]$ (Ref. 15) and our preliminary results for isotopic ZnSe based on PL measurements of the bound exciton (neutral acceptor I_1) $[\partial E/\partial M_{\mathrm{Se}} = 140 \pm 40\ \mu\mathrm{eV/amu}$ and $\partial E/\partial M_{\mathrm{Zn}} = 240 \pm 40\ \mu\mathrm{eV/amu}]$ which will be published in detail elsewhere.

Such behavior, however, is not found in wurtzite CdS. A

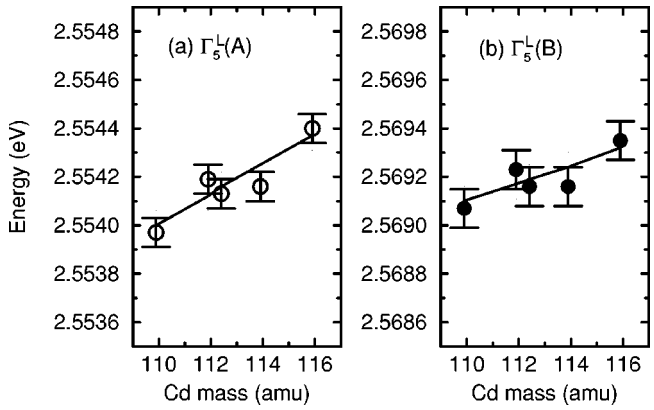

FIG. 5. Dependence of the ground-state energy of the $\Gamma_5^L(A)$ (a) and $\Gamma_5^L(B)$ excitons (b) on the isotopic mass of Cd obtained from PR measurements at 6 K. The solid lines represent the best fit with a straight line.

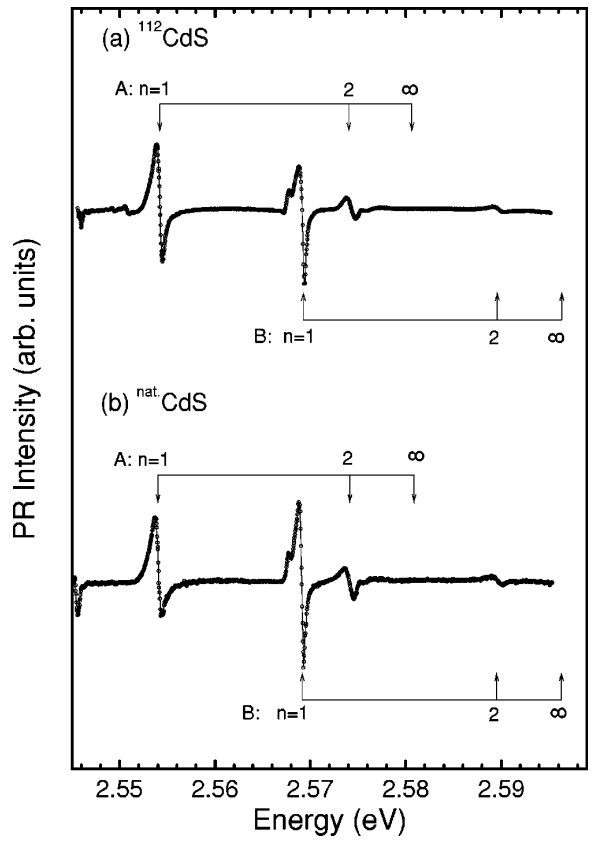

FIG. 6. PR spectra of (a) ^{112}CdS and (b) $^{nat.}$CdS at 6 K. The assignment of the spectral features to various components of the series of A and B excitons is indicated.

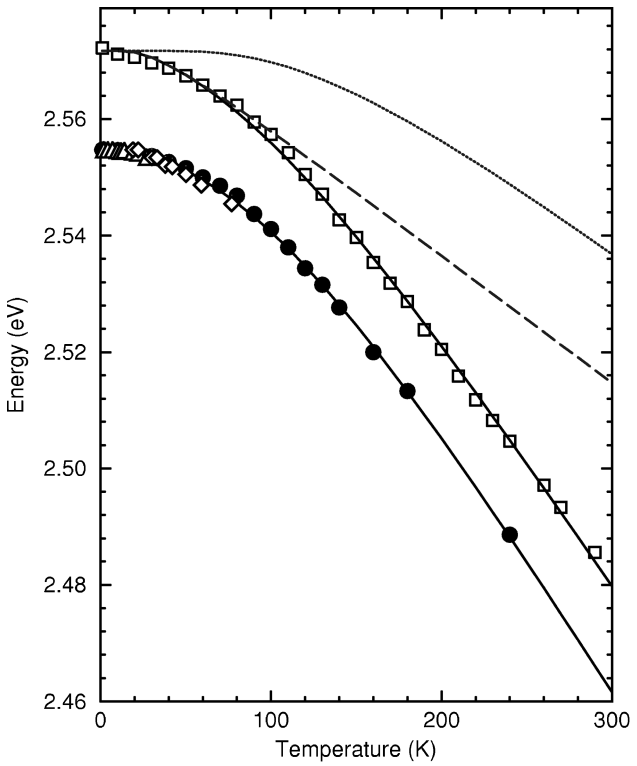

FIG. 7. Temperature dependence of the A and B excitons in CdS. The filled circles and open squares display wavelength-modulated reflectivity data (Ref. 24), while the diamonds and triangles represent the measured gap energy of the A band gap reduced by the exciton binding energy of 27 meV (from Refs. 25 and 26, respectively). The solid lines are least-squares fits to the data performed with Eq. (5) using the average phonon frequencies $\omega_{\mathrm{Cd}} = 60\ \mathrm{cm}^{-1}$ and $\omega_{\mathrm{S}} = 270\ \mathrm{cm}^{-1}$ (see text). The dashed and the dotted lines represent the individual contributions of acoustic phonons (Cd vibrations with average frequency ω_{Cd}) and optic phonons (S vibrations with average frequency ω_{S}) to the shift of the B exciton, respectively.

previous reflectivity and PL study[17] of $^{nat.}$Cd^{32}S and $^{nat.}$Cd^{34}S shows that for anion isotope substitution the ground state ($n = 1$) energies of both A and B excitons have a positive energy shift with the large rate of $\partial E/\partial M_{\mathrm{S}} = 740 \pm 100\ \mu$eV/amu. This value is more than one order of magnitude larger than $\partial E/\partial M_{\mathrm{Cd}}$ reported in the present work.

Equation (3) can be rewritten as[10,15]

$$\Delta E_{n\mathbf{k}}(T) = \int_0^\infty d\omega\, g^2F(\mathbf{k},n,\omega)[n_{\omega j}(T)+\tfrac{1}{2}], \qquad (4)$$

where $g^2F(\mathbf{k},n,\omega)$ is a temperature-independent electron-phonon spectral function of the phonon frequency ω. Contributions to this function arise from both acoustic and optic phonons. In CdS, acoustic and optic phonons are energetically well separated because of the large mass difference between Cd ($M_{\mathrm{Cd}} = 112.4$) and S ($M_{\mathrm{S}} = 32.1$).[23] The acoustic and the lowest optic branches correspond mainly to vibrations of Cd atoms while the remaining six high-frequency optic branches are dominated by the motions of the S atoms.[3,23] The DW contribution to the gap renormalization can be obtained from a pseudopotential band structure by replacing the atomic pseudopotentials V by $Ve^{-\frac{1}{6}G^2\langle u^2\rangle}$ (where G^2 is the squared magnitude of a reciprocal lattice vector and u the vibrational amplitude of the corresponding atom). This procedure is analogous to the introduction of Debye-Waller factors in either x-ray or neutron diffraction. The dependence of the gaps on temperature and isotopic mass is then derived from an expansion of the calculated gap energies to first order in the mean squared phonon displacement $\langle u^2\rangle \sim (\hbar/M\omega)(n+\frac{1}{2})$, which leads to

$$E(M,T) = \mathcal{E}_0 - \frac{a}{\omega_{\mathrm{Cd}}M_{\mathrm{Cd}}}[n(\omega_{\mathrm{Cd}},T)+\tfrac{1}{2}] - \frac{b}{\omega_{\mathrm{S}}M_{\mathrm{S}}}[n(\omega_{\mathrm{S}},T)+\tfrac{1}{2}], \qquad (5)$$

where $\mathcal{E}_0$ represents the unperturbed gap energy and the additional two terms on the right-hand side correspond to the contributions from the acoustic phonons (Cd vibrations) and optic phonons (S vibrations), respectively. Using an average acoustic-phonon frequency of $\omega_{\mathrm{Cd}} \simeq 60\ \mathrm{cm}^{-1}$ and an average optic-phonon frequency of $\omega_{\mathrm{S}} \simeq 270\ \mathrm{cm}^{-1}$,[23] a least-squares fit to experimental data of the temperature dependence of the A and B excitons in CdS,[24–26] as shown in Fig. 7, yields $a = 0.0134$ and $b = 0.1310\ \mathrm{eV}^2$ amu for the A exciton and $a = 0.0159$ and $b = 0.0999\ \mathrm{eV}^2$ amu for the B exciton, respectively. The zero-temperature isotopic-mass-dependent renormalization of the electron energies can also be predicted using Eq. (5). Using the approximate expression $\omega_{\mathrm{Cd(S)}} \propto 1/\sqrt{M_{\mathrm{Cd(S)}}}$ we find

$$\frac{\partial E}{\partial M_{\mathrm{Cd}}}=\frac{a}{4\omega_{\mathrm{Cd}}M_{\mathrm{Cd}}^2},\quad \frac{\partial E}{\partial M_{\mathrm{S}}}=\frac{b}{4\omega_{\mathrm{S}}M_{\mathrm{S}}^2}. \tag{6}$$

In this manner, we obtain $\partial E/\partial M_{\mathrm{Cd}} = 36\ \mu$eV/amu (42 μeV/amu) and $\partial E/\partial M_{\mathrm{S}} = 950\ \mu$eV/amu (724 μeV/amu) for the A (B) exciton, respectively. Given the simplified treatment of the CdS lattice dynamics by means of only two average oscillators (ω_{Cd}, ω_{S}), these values are in surprisingly good agreement with the results for isotope substitution of the Cd and S atoms listed in Table I.

In the Group IV and III-V semiconductors occupied d levels can be safely treated as part of the atomic cores. They are well below the valence band and thus have little influence on the optical properties near the gap.[27] Typical energy differences between the p valence band and the d bands are 32, 18, and 9 eV for the 3d electrons of Ge, Ga, and Zn atoms in Ge, GaAs, and ZnSe, respectively.[27] One can therefore neglect the d electrons of the cations when calculating the electronic structure and the influence of the electron-phonon interaction near the fundamental band gap. However, this situation changes if the energy difference between these core levels and the valence band becomes smaller.[28] In CdS the Cd 4d states lie only about 6 eV below the S 3p states, which provide the dominant contribution to the valence bands.[27,29] Hence, one would expect $3p-4d$ hybridization with some specific influence on the valence bands. It has indeed been reported that the Cd 4d ''core levels'' yield significant contributions to the optical properties of CdS in the region of interband transitions, and one has to include the p-d hybridization when calculating either the electronic band structures[29–31] or the vibrational properties.[23] The admixture of anion p and cation d states raises the energy of the top valence bands and thus decreases the gap.[14,16,28,29] Taking the electron-phonon interaction into account, an increase in temperature or, analogously, a decrease of the Cd mass at low temperature is expected to cause a reduction of the Debye-Waller factor $\approx 1-\frac{1}{6}\langle u^2\rangle G^2$ which, in turn, should weaken the p-d interaction.[2,14] As a result, a downshift of the top valence band should appear and compensate, at least partially, the conventional gap decrease due to the electron-phonon interaction acting on the s-like conduction and p-like valence gap states.

In empirical pseudopotential calculations for CuCl, it has been shown that the p-d hybridization is not affected by isotopic substitution of anion atoms while it results in an anomalous *negative* value of $\partial E/\partial M_{\mathrm{Cu}}$.[14] In analogy to this effect, a much smaller gap shift (although of the standard sign) is also observed in CdS with increasing the Cd mass compared to that observed when changing the S mass. In the I-VII compound CuCl the d levels are even closer in energy to the Cl-derived p-like valence band (as close as 1 eV) (Ref. 32) and their spatial extent is larger. The p and d levels in CuCl therefore hybridize more strongly. As a consequence, the increase of the CuCl gap with increasing Cu mass, expected by analogy with other zinc-blende-type semiconductors, is *overcompensated* by the effect of the electron-phonon interaction on the p-d mixing. Therefore the gap of CuCl anomalously *decreases* with either an *increase* of the Cu mass or a *decrease* in temperature.[2,14,16] In CdS one would expect this effect to be smaller since the Cd 4d levels are farther below the top of the valence band than in the copper halides. Nevertheless, some influence of the electron-phonon interaction on the p-d hybridization should still be observable. This is confirmed by our experimental results for both the isotope-mass and the temperature effects on the gap. The 4d-electron contribution results in a reduction of the effect due to acoustic phonons but, contrary to the case of CuCl,[2,14,16] does not suffice to reverse the sign of the gap shift. We consider this to be one in a class of effects of semicore d electrons on semiconductor band structures.

IV. CONCLUSION

In conclusion, we have observed the effect of changing the isotopic mass of Cd on the A and B excitons in isotopically pure ^{110}CdS, ^{112}CdS, ^{114}CdS, ^{116}CdS, and natural CdS using PL, PR, and PzR spectroscopies. With increasing Cd mass the A exciton increases at a rate of 68 μeV/amu while the B exciton changes by 40 μeV/amu. These values are significantly smaller than the corresponding shift $\partial E/\partial M_{\mathrm{S}} = 740 \pm 100\ \mu$eV/amu, which has been reported previously.[17] A fit of the temperature dependence of the exciton energies with a phenomenological model yields results that are remarkably consistent with the isotope effects. The origin of the very small value of $\partial E/\partial M_{\mathrm{Cd}}$ revealed by both the dependence of the gap on the isotopic mass and on the temperature is traced back to the influence of Cd 4d electrons on the valence-band p states, in analogy to earlier findings for CuCl. In both semiconductors the electron-phonon interaction affects the p-d hybridization, which causes an additional contribution to the gap shift of a sign opposite to the standard one.

ACKNOWLEDGMENTS

We thank M. Siemers, H. Hirt, and P. Hießl for technical assistance. J.M.Z. gratefully acknowledges financial support from the Max-Planck-Gesellschaft. Thanks are also due to A. Debernardi for a careful reading of the manuscript.

*Present address: The University of British Columbia, Department of Electrical Engineering, Vancouver, B.C., Canada V6T 1Z4.

[1] M. Cardona, in *Festkörperprobleme: Advances in Solid State Physics*, edited by R. Helbig (Vieweg, Braunschweig, 1994), Vol. 34, p. 35.

[2] T. Ruf, A. Göbel, M. Cardona, C. T. Lin, J. Wrzesinski, M. Steube, K. Reimann, N. Garro, A. Cantarero, J.-C. Merle, and M. Joucla, in *The Physics of Semiconductors*, edited by M. Scheffler and R. Zimmermann (World Scientific, Singapore, 1996), p. 185.

[3] J. M. Zhang, T. Ruf, A. Göbel, A. Debernadi, R. Lauck, and M. Cardona, *The Physics of Semiconductors* (Ref. 2), p. 201.

[4] A. Göbel, T. Ruf, C. T. Lin, M. Cardona, J.-C. Merle, and M. Joucla, Phys. Rev. B **56**, 210 (1997).

[5] J. M. Zhang, T. Ruf, M. Cardona, O. Ambacher, M. Stutzmann, J.-M. Wagner, and F. Bechstedt, Phys. Rev. B **56**, 14 399 (1997).
[6] P. B. Allen, Philos. Mag. B **70**, 527 (1994).
[7] P. B. Allen and M. Cardona, Phys. Rev. B **27**, 4760 (1983).
[8] P. Lautenschlager, P. B. Allen, and M. Cardona, Phys. Rev. B **31**, 2163 (1985).
[9] S. Gopalan, P. Lautenschlager, and M. Cardona, Phys. Rev. B **35**, 5577 (1987).
[10] S. Zollner, M. Cardona, and S. Gopalan, Phys. Rev. B **45**, 3376 (1992).
[11] P. Etchegoin, J. Weber, M. Cardona, W. L. Hansen, K. Itoh, and E. E. Haller, Solid State Commun. **83**, 843 (1992).
[12] C. Parks, A. K. Ramdas, S. Rodriguez, K. M. Itoh, and E. E. Haller, Phys. Rev. B **49**, 14 244 (1994).
[13] T. Ruf, M. Cardona, H. Sternschulte, S. Wahl, K. Thonke, R. Sauer, P. Pavone, and T. R. Anthony, Solid State Commun. **105**, 311 (1998).
[14] N. Garro, A. Cantarero, M. Cardona, T. Ruf, A. Göbel, C. Lin, K. Reimann, S. Rübenacke, and M. Steube, Solid State Commun. **98**, 27 (1996).
[15] N. Garro, A. Cantarero, M. Cardona, A. Göbel, T. Ruf, and K. Eberl, Phys. Rev. B **54**, 4732 (1996).
[16] A. Göbel, T. Ruf, M. Cardona, C. T. Lin, J. Wrzesinski, M. Steube, K. Reimann, J.-C. Merle, and M. Joucla (unpublished).
[17] F. I. Kreĭngol'd, K. F. Lider, and M. B. Shabaeva, Fiz. Tverd. Tela (Leningrad) **26**, 3490 (1984) [Sov. Phys. Solid State **26**, 2102 (1985)].
[18] A. Gavini and M. Cardona, Phys. Rev. B **1**, 672 (1970).
[19] T. Ruf, R. T. Phillips, A. Cantarero, G. Ambrazevičius, M. Cardona, J. Schmitz, and U. Rössler, Phys. Rev. B **39**, 13 378 (1989).
[20] F. H. Pollak and H. Shen, Superlattices Microstruct. **6**, 203 (1989).
[21] *Physics of Group II-VI Elements and I-VII Compounds*, edited by O. Madelung, M. Schulz, and H. Weiss, Landolt-Börnstein, New Series, Group III, Vol. 17, Pt. b (Springer, Berlin, 1982); *Semiconductors Intrinsic Properties of Group IV Elements nad III-V Compounds*, edited by O. Madelung *et al.* Landölt-Börnstein, New Series, Group III, Vol. 22, Pt. a (Springer, Berlin, 1987).
[22] The hydrogenic model should, in principle, be modified in wurtzite crystals because of the anisotropy of the effective-mass and the dielectric constant. See W. Shan, B. D. Little, A. J. Fischer, J. J. Song, B. Goldenberg, W. G. Perry, M. D. Bremser, and R. F. Davis, Phys. Rev. B **54**, 16 369 (1996).
[23] A. Debernardi, N. M. Pyka, A. Göbel, T. Ruf, R. Lauck, S. Kramp, and M. Cardona, Solid State Commun. **103**, 297 (1997).
[24] A. Anedda and E. Fortin, Phys. Status Solidi A **36**, 385 (1976).
[25] D. G. Seiler, D. Heiman, R. Feigenblatt, R. L. Aggarwal, and B. Lax, Phys. Rev. B **25**, 7666 (1982).
[26] C. Benoit à la Guillaume, J.-M. Debever, and F. Salvan, Phys. Rev. **177**, 567 (1969).
[27] *Photoemission in Solids I*, edited by M. Cardona and L. Ley, Topics in Applied Physics Vol. 26 (Springer, Berlin, 1978); *Photoemission in Solids II*, edited by L. Ley and M. Cardona, Topics in Applied Physics Vol. 27 (Springer, Berlin, 1979).
[28] M. Cardona, Phys. Rev. **129**, 69 (1963).
[29] K. J. Chang, S. Froyen, and M. L. Cohen, Phys. Rev. B **28**, 4736 (1983).
[30] S.-H. Wei and A. Zunger, Phys. Rev. B **37**, 8958 (1988).
[31] D. Vogel, P. Krüger, and J. Pollmann, Phys. Rev. B **52**, 14 316 (1995).
[32] A. Goldmann, Phys. Status Solidi B **81**, 9 (1977).